Design of Nanosecond-Scale High-Voltage Switching Circuit for Pockels Cell-Based Q-Switching Lasers

Mehdi Keikha, Abolfazl Abedi, and Reza Massudi

Laser and Plasma Research Institute, Shahid Beheshti University, Tehran, Iran

Corresponding author email: mehdikeikha.op@gmail.com

Received: Apr. 13, 2025, Revised: Sept. 02, 2025, Accepted: Sept. 07, 2025, Available Online: Sept. 09, 2025,
DOI: 10.61186/ijop.18.1.85

ABSTRACT— Electro-optic modulators are essential components in many optical systems, including laser amplifiers, Q-switching for pulsed lasers, pulse pickers for ultrafast laser systems, and pulse reshaping. Pockels cells, as the active components in an electro-optic modulator, require an electronic circuit capable of fast and clean high-voltage switching. In this paper, we report a suitable electronic circuit consisting of a chain of MOSFET transistors and evaluate its performance in terms of switching speed and precision. The results demonstrate that this circuit can generate high-voltage pulses with low power loss, rise times in the nanosecond range, and fall times in the microsecond range. Therefore, the proposed circuit can meet the diverse demands of advanced optical systems, particularly Q-switched lasers. The advantages and limitations of the circuit are analyzed, and some other potential applications are also suggested.

KEYWORDS: Electro-optic modulators, Fast high voltage switching, MOSFET chain, Pockels cell, Q-switched lasers.

I. INTRODUCTION

Electro-optic modulators are devices capable of altering the properties of light, such as phase, amplitude, or polarization, by applying an electric field to a special crystal. Each crystal has its own properties based on its electro-optic coefficient, half-wave voltage, damage threshold, temperature stability, and transmission range [1]. They can be utilized for various applications, including Q-switching, pulse picking, amplitude and phase modulation, and polarization rotation. To operate a Pockels cell, an appropriate electronic circuit is required to generate high-voltage pulses in the kilovolt range with fast rise and fall times. The required voltage depends on the type and length of the crystal as well as the intended application [2]. Generating and switching such pulses necessitate high-power and high-speed electronic components such as avalanche transistors, IGBTs, power MOSFETs, microwave triodes [3]. Power MOSFETs are capable of producing signals with amplitudes in the range of hundreds of volts and rise and fall times in the nanosecond range [4]. In the past, vacuum tubes or microwave triodes were commonly used in high-voltage electronic circuits for fast switching operations [5], [6]. However, due to their bulkiness and unsuitability for high-frequency applications, they were replaced by MOSFETs. The advantages of using MOSFETs include longer lifespan, lower power dissipation, and faster switching speeds. Furthermore, MOSFETs have a faster turn-on speed compared to IGBTs and a higher maximum voltage threshold than avalanche transistors [7], [8]. However, in high-voltage applications, to increase the voltage threshold, a specific number of MOSFETs must be connected in series. As a result, power MOSFETs can be used in series for fast switching between high voltages, which is required in experiments such as beam modulation in an electro-optic modulator [4]. The primary challenge in switching a MOSFET chain is the simultaneous and high-speed turn-on of the MOSFETs to achieve a fast rise time. Each MOSFET requires the application of gate-source voltage pulses with an amplitude greater than the threshold voltage ($V_{GS} \geq V_{th}$) for

[Downloaded from ijop.ir on 2026-11-23]

proper turn-on. One method for simultaneously turning on multiple series-connected MOSFETs involves using multiple transformers to drive the MOSFET gates while isolating the gate drive section from high voltages [9]. In fast switching of multiple MOSFETs with this method, challenges such as instantaneous voltage spikes at the MOSFET gate-source terminals (due to an LC resonant frequency caused by the combination of the transformer's inductance and the MOSFET gate-source capacitance), transformer core saturation (leading to a sudden increase in MOSFET current and potential damage), and the risk of desynchronization in triggering all MOSFETs simultaneously arise. Overcoming these challenges often requires additional components or circuits, which at best results in a bulkier and more expensive circuit design [10]. An alternative circuit design for driving multiple series-connected MOSFETs that is more compact, cost-effective, and geometrically simpler was reported by Baker and Hess [4], [9]. In their method, triggering the first MOSFET sequentially activates the entire MOSFET chain in a cascading manner. In this paper, the performance of series-connected power MOSFETs is analyzed to enhance their effective hold-off voltage. In Q-switched pulsed laser operation, the electronic switch is activated by a rectangular control pulse consisting of a rise time, pulse width, and fall time. The removal of cavity losses and the generation of the laser pulse occur precisely during the rise time of the control pulse, while the pulse width and fall time have minimal impact on this process. Therefore, the rise time of the control pulse is the critical factor in determining the characteristics of the laser pulse [11], [12]. This study focuses on generating high-voltage pulses with fast rise times and discusses the challenges encountered in designing and constructing a suitable pulse generator circuit for driving a Pockels cell.

II. THEORY

For a traveling wave in an arbitrary direction in an anisotropic crystalline medium, there are generally two orthogonally polarized modes. The polarization and refractive indices of these two modes can be determined using the refractive index ellipse [13]. The equation of the refractive index ellipse under the influence of an electric field is as follows [14], [15]:

$$\frac{x_1^2}{n_1^2}+\frac{x_2^2}{n_2^2}+\frac{x_3^2}{n_3^2}+A_1x_1^2+A_2x_2^2+A_3x_3^2 +2A_4x_2x_3+2A_5x_3x_1+2A_6x_2x_1=1 \quad (1)$$

The linear change in the coefficients A_I due to an arbitrary electric field $\mathbf{E}(\mathrm{E_x},\mathrm{E_y},\mathrm{E_z})$ is described as:

$$A_I=\sum_{k=1}^{3} r_{Ik}E_k \quad (2)$$

where r_{Ik} represents the components of the electro-optic tensor of a specific crystal belonging to certain crystal group. in summation over k, the convention $1=x$, $2=y$, and $3=z$ is used where the axes x, y, z are considered parallel to the principal axes of the crystal). The terms multiplied by the coefficients A_I (combinations of x_1, x_2, x_3) indicate the deformation, size, or orientation of the refractive index ellipsoid caused by the applied electric field. By specifying the light propagation direction, the principal axes of the crystal, and the refractive indices along these axes (n_1 , n_2 , and n_3) in the absence of an electric field, and substituting the constants r_{Ik} ,for the specific crystal, into Eq. (2) and by diagonalizing Eq. (1), the principal axes of the modified refractive index ellipsoid under the influence of the electric field, as well as the principal refractive indices $n_1(E)$, $n_2(E)$, and $n_3(E)$, can be determined. Finally, the refractive indices corresponding to the orthogonal modes can be calculated.

Thus, for a light wave propagating along the z-axis through a Pockels cell with an applied electric field **E**, the orthogonal modes propagate at different velocities, $c_0/n_1(E)$ and $c_0/n_2(E)$. These two modes, after propagating a distance L within the length of the crystal,

[Downloaded from ijop.ir on 2026-11-23]

acquire a relative phase delay due to the Pockels effect given by:

$$\varphi = \Delta n(E)k_0 L = \varphi_0 - \frac{1}{2}k_0(r_1 n_1^3 - r_2 n_2^3)EL \qquad (3)$$

where r_1 and r_2 are the appropriate Pockels coefficients and φ_0 is the phase retardation in the absence of the electric field. If E is generated by applying a voltage V between two surfaces of the crystal separated by a distance d, the phase of a light wave can be altered by changing the applied voltage. Such a medium acts as a dynamic wave retarder with electrically tunable properties. According to Eq. (3), the voltage required to create a phase delay of π is:

$$V_{\lambda/2} = \frac{d}{L}\frac{\lambda_0}{r_1 n_1^3 - r_2 n_2^3} \qquad (4)$$

The parameter $V_{\lambda/2}$ is known as the half-wave voltage. The electric field can be applied in two configurations: longitudinal, where the electric field is parallel to the direction of light propagation ($d = L$), and transverse, where the electric field is perpendicular to the direction of light propagation. Longitudinal Pockels cells have lower losses and scattering compared to transverse Pockels cells but require higher voltages.

The half-wave amplitude and quarter-wave voltage amplitude (half of the voltage required to induce a π/2 delay) applied to the Pockels cell are on the order of one to several kilovolts. For example, when using a KD*P crystal as a half-wave retardation plate in the longitudinal configuration, according to Eq. (4), the required voltage at a wavelength of 546nm is 2.98kV. The timing, speed, and precision of applying this voltage determine the quality of the modulator, necessitating an electronic circuit capable of high-speed switching of high voltages.

III. Circuit Simulation

The designed circuit has been simulated in the Capture environment of PSpice software, as shown in Fig. 1. This circuit is divided into four main sections: the DC source (V1), the charging capacitor (C1), the switch (consisting of a series assembly of IRFAF52 MOSFET transistors), and the output load, which includes RL and the KD*P crystal (which usually has an internal resistance of approximately 10MΩ and a capacitance of approximately 6pF [16]).

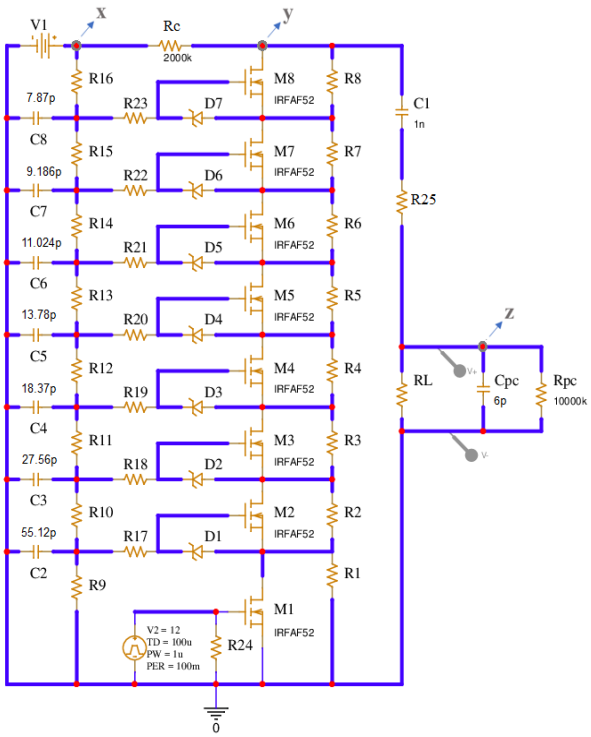

Fig. 1. The high-voltage circuit designed for switching the KD*P Pockels cell.

When the switch is off, the DC source charges the capacitor C1. When the switch is turned on, the charge stored in the capacitor is discharged onto the crystal as a high-voltage pulse**.** Therefore, the circuit operates in two stages: the "off" state and the "on" state. In the "off" state, when the control pulse ($V2$) from the driver has not yet reached the circuit, all MOSFETs (M1 to M8) are off. Capacitor C1 is charged through resistor R_C, and the supply voltage is distributed across resistors R1 to R8 to provide the drain-source voltage (V_{DC}) for the MOSFETs and to charge capacitors C2 to C8. To ensure that the MOSFETs remain off during the switch's off state, a voltage division method is employed. This is achieved by placing resistors R9 to R16 in parallel with capacitors C2 to C8 and creating a voltage imbalance across the Zener diodes. This imbalance in voltage division is

[Downloaded from ijop.ir on 2026-11-23]

established by selecting a value for resistor R9 lower than that of resistor R1 (such that R1=R9+ΔR), while the equivalent resistance of the two branches remains the same. Consequently, the anode voltage of Zener diode D1 exceeds its cathode voltage ($V_A > V_K$). Since $V_{GS} = V_G - V_S = V_K - V_A$, it can be concluded that a negative voltage is applied to the gate-source junction of the MOSFETs during the switch's off state. Therefore, the current flowing through the MOSFETs and the circuit's output voltage will also be zero.

In the "on" state, as soon as the control pulse V2 reaches its high level (+12V), M1 is initially turned on ($V_{GS}1 \geq V_{th}$). The drain-source current is established, and its voltage rapidly decreases, i.e., the drain terminal is grounded, subsequently reducing the source potential of transistor M2. Similarly, transistors M3, M4, and so on, are sequentially turned on at nanosecond intervals. In effect, at the instant of switching, the Zener diodes are reverse biased and act as a voltage source with a voltage V_Z to provide the gate voltage for the MOSFETs, thereby turning them on. The Zener diodes' voltage V_Z and the capacitance of capacitors C2 to C8 provide the necessary charge for charging the gate-source capacitance of MOSFETs M2 to M8, thus activating the switch. The Zener diode employed, when reverse biased, exhibits a voltage $V_Z = 15V$, and when forward biased, a voltage $V_F = V_D^{ON} = 0.75V$. Therefore, during the switch's on state, the Zener diodes provide the necessary voltage (15V) to turn on MOSFETs M2 to M8 and protect the MOSFETs by limiting the maximum V_{GS} voltage to 15V (the maximum tolerable V_{GS} voltage of the MOSFET used in this circuit is 30V.). It is noteworthy that the capacitance of capacitors C2 to C8 is selected such that the application of gate-source voltage (V_{GS}) to the transistors occurs sequentially, with M2 turning on before M3, M3 before M4, and so on.

Another consideration in the discharge path of capacitors C2 to C8 is preventing the Zener diodes from overheating and damage due to the instantaneous current flowing through them after charging the gate capacitance of the MOSFETs. Indeed, at the switching instant, the voltage stored in capacitors C2 to C8 abruptly moves towards the Zener diodes with a peak current, potentially damaging the diodes. By placing small current-limiting resistors (R17 to R23) in the capacitors' discharge path before the Zener diodes, we prevent their damage.

Finally, with all MOSFETs turned on, the switch section is grounded, and the charge stored in capacitor C1 moves towards RL as a high-voltage negative pulse.

IV. RESULTS

The high-voltage pulses applied to the Pockels cell (comprising Rpc and Cpc) can be observed at the output of the designed circuit by connecting a probe across the Pockels cell. As illustrated in Fig. 2, for DC voltages of V1=3, 5, and 7kV, the circuit is capable of generating pulses with approximate amplitudes of 2.5, 4.2, and 5.8kV, respectively.

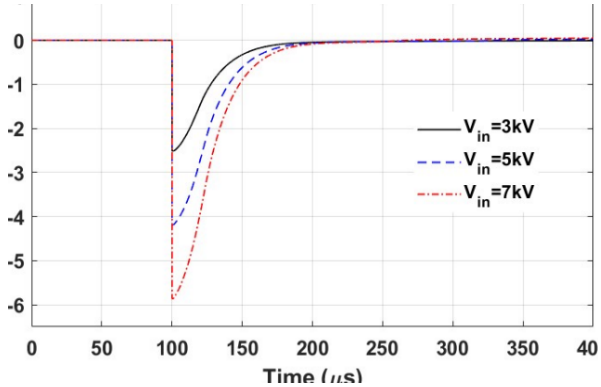

Fig. 2. Generated pulses at supply voltages of 3, 5, and 7kV.

The difference between the output voltage (the generated pulse amplitude) and the supply voltage results from voltage division across the specified resistances and capacitor C1. Figure 3 illustrates the voltage at three points x, y, and z for a supply voltage of 3.57kV. The voltage stored in capacitor C1 (at point y) is approximately 2.98kV and the output pulse amplitude is -2.98kV. Before switching, the positive terminal of the capacitor is at +Vy, while the other terminal is at 0V. Since the charge stored in the capacitor must remain constant, when the switch is applied, the positive terminal is brought to 0V and the other

[Downloaded from ijop.ir on 2026-11-23]

terminal, which is connected to the load, attains a negative potential relative to it (-Vy).

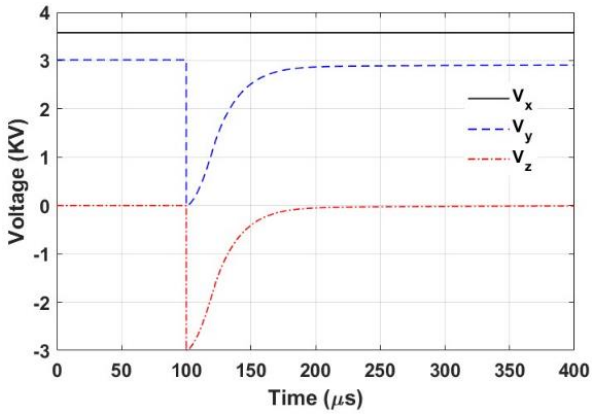

Fig. 3. The voltages at the three points x, y and z from the designed circuit shown in Fig. 1.

To further analyze the temporal development of the output pulse, the drain-source voltages of the series-connected MOSFETs during switching are shown in Fig. 4. As illustrated, the MOSFETs are sequentially turned on, resulting in a stepwise decrease in drain voltage from M1 to M8. This cascaded activation mechanism ultimately generates the output pulse across the Pockels cell. The fall time of the output pulse is governed by the switching behavior of the last MOSFET (M8), as seen in the timing of its voltage transition.

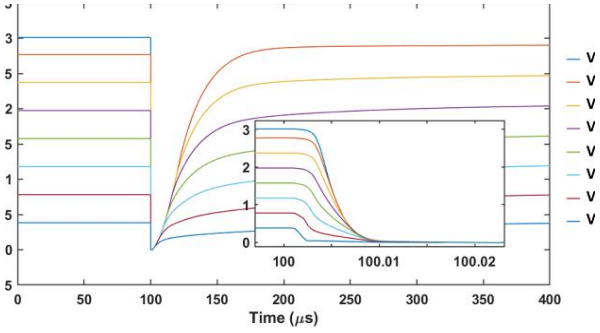

Fig. 4. Drain voltages of the cascaded MOSFETs at the moment of switching, illustrating the sequential turn-on behavior and the stepwise voltage drop across the series.

A closer examination of the zoomed-in switching waveform presented in Fig. 4 reveals that the MOSFETs are activated sequentially; however, this activation is not strictly serial in the sense that each transistor must fully switch before the next begins. Instead, after each MOSFET starts conducting, the subsequent stage initiates its turn-on process with a delay of approximately 1ns. This temporal overlap in switching events effectively reduces the total rise time of the output pulse compared to the sum of the individual transistor rise times. According to Fig. 5, the rise time of the generated pulses is approximately 20ns, while the fall time is on the order of microseconds (Note that the rise time of the pulse is displayed as descending due to the negative voltage polarity).

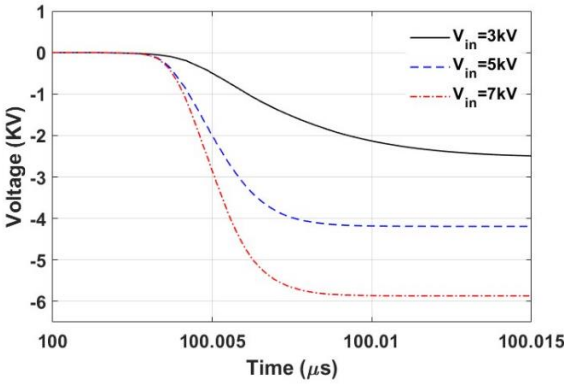

Fig. 5. Rise time of the generated pulses in Fig. 2.

The repetition rate of these pulses can be adjusted by tuning the repetition rate of the applied trigger pulse (V2), which, in this case, is set to 10Hz. It was determined that capacitor C1 is charged through resistor Rc, meaning that after five time constants ($\tau_C = R_C \times C1 = 2ms$), the capacitor becomes almost fully charged. Consequently, at repetition rates exceeding 100Hz ($1/(5\times 2ms)$), the switching efficiency decreases. Therefore, the optimal switching performance of the circuit is achieved at repetition rates below 100Hz.

V. DISCUSSION

The performance of the designed circuit in the simulation environment is nearly ideal; however, in practical implementation, certain considerations must be taken into account. Five key factors are highlighted below:

A. *Voltage Limitation*

The circuit supply voltage must not be high enough for the divided voltage across the drain-source terminals of the MOSFETs to exceed their maximum drain-source voltages threshold. In the designed circuit, the drain-

[Downloaded from ijop.ir on 2026-11-23]

source breakdown voltage of the MOSFETs is 900V. Therefore, the circuit supply voltage can theoretically be increased up to 7kV. However, in practical designs of pulse generator circuits suitable for driving Pockels cells, several challenges arise due to the need for high operating voltages, fast switching speeds, and circuit miniaturization. These challenges include phenomena such as corona discharge and flashover. In practice, when the voltage gradient on a conductor exceeds the dielectric strength of the surrounding air, the air becomes ionized. This phenomenon can lead to a partial discharge of electrical energy, known as corona discharge. Another hazardous phenomenon in electrical systems is flashover, in which the electric current deviates from its intended path and jumps through the air from one conductor to another or to the ground. Flashover occurs when the insulation between conductors is not sufficient to withstand the applied voltage, resulting in electrical breakdown. To mitigate these issues in pulse generator circuit design, two key considerations must be observed:

1. Maximizing the spacing between wires and terminals in the designed circuit board (and also the spacing between the terminals connected to the electrodes of the Pockels cell).

2. Reducing the supply and operational voltages in the circuit to lower levels, if possible.

B. *LC Resonant Frequency*

In the design of a high-voltage pulse generator for driving a Pockels cell, parasitic effects from wiring and circuit components pose significant challenges. At high frequencies, wires exhibit inductive behavior, while the Pockels cell acts as a capacitive load. Since the simulation environment is idealized, an inductor was deliberately added to the circuit's output to observe LC resonance, resulting in voltage overshoot at the pulse leading edge due to stored reactive energy. As shown in Fig. 6, this resonance effect increases the output voltage amplitude, which, if uncontrolled, may damage the Pockels cell and distort the waveform.

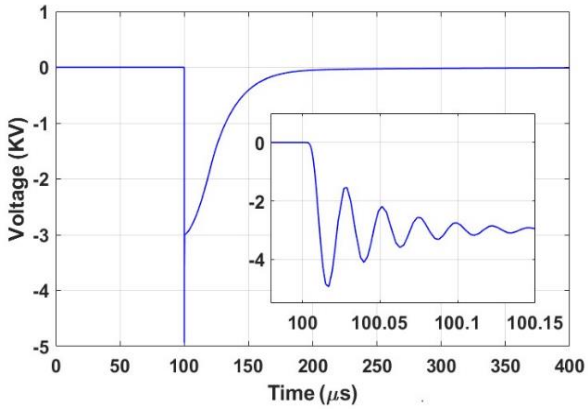

Fig. 6. Voltage overshoot generated at the pulse edge due to LC resonance of the wires and the Pockels cell.

To mitigate this, damping resistors were introduced to suppress oscillations by increasing the damping factor and dissipating excess energy. Figure 7 illustrates how the resistors effectively stabilize the voltage by reducing unwanted oscillations. Proper resistor selection, along with optimized pulse current routing and minimized wiring length, is essential for ensuring circuit stability and preventing resonance-related issues.

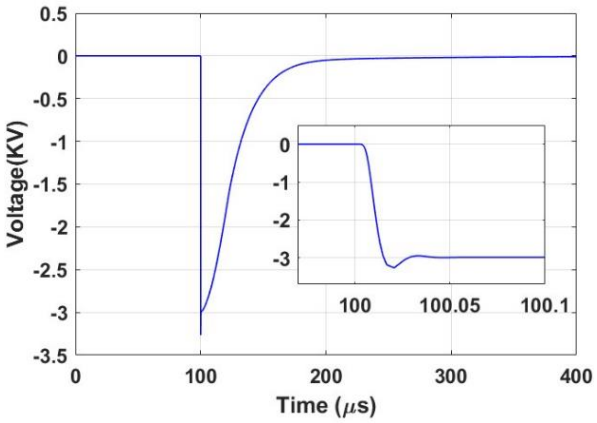

Fig. 7. Damping of the resonance generated at the pulse edge by series connection of appropriately selected resistors at the circuit output.

Although LC resonance can be undesirable or even detrimental, in certain cases, the use of a properly selected inductor can be beneficial. Specifically, in high-voltage pulse generator circuits, the presence of an inductor at the output, in conjunction with the capacitive properties of the Pockels cell, can induce a controlled resonance. This resonance leads to an increased voltage amplitude at the rising edge of the pulse, enhancing the optical

[Downloaded from ijop.ir on 2026-11-23]

switching performance of the Pockels cell. Importantly, this voltage amplification occurs locally within the Pockels cell and does not propagate throughout the entire circuit, thereby preventing excessive voltage buildup and mitigating the risks of corona discharge or flashover. From a design perspective, this approach offers two primary advantages. First, by generating a controlled resonance at the pulse rise time, the response time of the Pockels cell is optimized, thereby improving pulse conversion efficiency. Second, by carefully tuning the LC parameters, the resonance frequency can be confined to a stable and predictable range, reducing unwanted electromagnetic noise and enhancing the overall system stability. Consequently, this technique serves as an effective strategy for optimizing high-voltage pulse generator circuits, minimizing electrical stress on circuit components, and prolonging the operational lifespan of optoelectronic elements.

C. *Impedance Matching*

In circuits where the output pulse is transmitted to the Pockels cell via a cable, achieving short transmission times requires impedance matching between the cable resistance R and the capacitance C of the Pockels cell (to achieve a short time constant $\tau = RC$). Additionally, in practice, the control pulse applied to the circuit is not perfectly rectangular. In some cases, unintended voltage components with inverse polarity may appear at the edges of the generated pulse, known as voltage reflections or undershoot. These undershoots result from impedance mismatch and voltage reflections. To mitigate this issue, specific resistance values should be used at the circuit input to match the input impedance with the cable impedance. Furthermore, at the circuit output, a diode-based clipping circuit utilizing high-power diodes can be implemented to eliminate unwanted inverse voltage components.

D. *Selection of Suitable Components*

In designing and constructing the Pockels cell driver circuit, it is essential to use compact components to achieve a smaller and more integrated circuit. Additionally, these components must be fast, capable of handling high power, and ideally require minimal or no cooling systems. The IRFAF52 transistor comes in a TO-3 package, which is bulkier compared to MOSFETs with a TO-220 package. A more suitable alternative in practice would be modern MOSFETs such as BUK456 and K3532. These MOSFETs are both fast and compact. However, their rapid switching requires efficient charging of the gate-to-source capacitance within short time intervals. As mentioned earlier, M1 must turn on before M2, M2 before M3, and so on. The approach used in this study is a stepwise reduction of the capacitance values of C2 to C8 according to the relation $Ci = C2 / (i - 1)$, where i=2,3,...,8 .

E. *Noise Considerations in Circuit*

As discussed earlier, high-speed switching of high voltages on nanosecond time scales can generate various forms of electrical noise, potentially disrupting the stable operation of the driver circuit and interfering with nearby optical or electronic components. In addition to the resonance-induced voltage overshoot described in the LC resonance section, the system is susceptible to other types of electromagnetic interference (EMI), including radiated and conducted noise. These noise components are particularly pronounced due to the fast rise time (~20 ns) and high voltage levels used in the circuit.

A primary source of radiated noise is the rapid current transitions (high di/dt) in the discharge path of the main capacitor, which can produce significant high-frequency electromagnetic radiation. Additionally, capacitive or inductive coupling between the high-voltage switching stage and sensitive control or triggering lines may cause instability or false triggering. Voltage reflections due to impedance mismatches, particularly at the interface with the capacitive load (e.g., the Pockels cell), can further distort the desired pulse shape, leading to undershoots or ringing.

To address these challenges, several practical design strategies should be implemented. First, careful printed circuit board (PCB) layout is critical: high-current paths should be

[Downloaded from ijop.ir on 2026-11-23]

minimized, ground return paths optimized to reduce loop areas, and signal lines routed away from high-voltage switching nodes. Second, enclosing the high-voltage section within a grounded metallic shield can significantly reduce radiated EMI. Shielded cables should be used for connections to external components, such as the Pockels cell.

Furthermore, EMI filters on the power supply and trigger input lines can mitigate conducted noise, while impedance matching between the output stage and the electro-optic load can minimize voltage reflections. Clamping diodes can suppress transient overshoots, and employing soft-switching or slew-rate-limited gate drivers can reduce radiated emissions without compromising switching speed. Finally, physically and electrically isolating the gate-drive circuitry from the main switching stage helps maintain signal integrity and minimizes mutual interference.

By incorporating these design considerations, the adverse effects of noise in high-voltage pulse generators can be significantly reduced, resulting in more robust and reliable performance for electro-optic applications.

VI. CONCLUSION

In this study, a high-voltage pulse generator circuit was designed and analyzed, demonstrating its capability to perform fast high-voltage switching with a nanosecond-scale rise time. A key feature of this circuit is its adjustable output voltage amplitude, which can be modified by altering the circuit components to suit specific applications. This flexibility makes the circuit particularly suitable for various optoelectronic and laser switching applications. For instance, when the circuit output is applied to a longitudinally biased KD*P crystal, it can function as a half-wave retarder in optical systems, such as Q-switches for pulsed lasers. Additionally, this circuit is well-suited for switching operations in regenerative amplifier cavities with low repetition rates. One of the major advantages of this design is that it eliminates the need for heat sinks or additional cooling mechanisms for critical components, particularly MOSFETs, thereby enhancing efficiency, reducing costs, and optimizing circuit size. Furthermore, this study also investigated practical challenges and limitations that may arise in practical implementations beyond theoretical simulations. By incorporating these considerations into the fabrication process and synchronizing the Q-switching operation with the flash lamp via the driver circuit, it is possible to achieve an optimized pulsed laser system suitable for various industrial and scientific applications.

REFERENCES

[1] R. Paschotta, Encyclopedia of Laser Physics and Technology. New York:Wiley, 2008.

[2] A. Ashkin, C. Boyd, and T. Dziedzic, “Photorefractive effect in crystals,” Appl. Phys. Lett., Vol. 9, pp. 72–80, 1966.

[3] S. Rukin, “Pulsed power technology based on semiconductor opening switches: A review,” Rev. Sci. Instrum., Vol. 91, p. 011501(1-47), Jan. 2020.

[4] R. Baker and B. Johnson, “Series operation of power MOSFETs for high-speed, high-voltage switching applications,” Rev. Sci. Instrum., Vol. 64, pp. 1655–1656, July 1993.

[5] J. Grenier, S. Jayaram, A. El-Hag, and M. Kazerani, “A study on effect of medium conductivity on its electric strength under different source conditions in nanosecond regimes,” in Proc. IEEE Int. Conf. Dielectric Liquids, pp. 261–264, 2005.

[6] J.L. Hudgins and W.M. Portnoy, “High di/dt pulse switching of thyristors,” IEEE Trans. Power Electron., Vol. PE-2, No. 2, pp. 143–148, 1987.

[7] L. Lorenz, “Study of the switching performance of a power MOSFET circuit,” in Proc. IEEE Power Electron. Spec. Conf, New York, pp. 215–224, June 1984.

[8] S. Frankeser, H. Muhsen, and J. Lutz, “Comparison of drivers for SiC-BJTs, Si-IGBTs and SiC-MOSFETs,” in Proc. PCIM Europe 2015; Int. Exhib. and Conf. Power Electron., Intelligent Motion, Renewable Energy and Energy Management, pp. 1–9, May 2015.

[9] X.W. Feng, X.W. Long, and Z.Q. Tan, “Nanosecond square high voltage pulse

[Downloaded from ijop.ir on 2026-11-23]

generator for electro-optic switch," Rev. Sci. Instrum., Vol. 82, No. 7, p. 075102(1-4), July 2011.

[10] M. Keikha, "Design and construction of Pockels cell driver to create adjustable delay with voltage in laser," M.S. thesis, Laser Research Institute, Shahid Beheshti Univ., Tehran, Iran, 2024.

[11] W. E. White, J. R. Hunter, L. Van Woerkom, T. Ditmire, and M. D. Perry, "120-fs terawatt Ti:Al_2O_3/Cr:$LiSrAlF_6$ laser system," Opt. Lett., Vol. 17, No. 15, pp. 1067–1069, Aug. 1992.

[12] J.P. Salvestrini, M. Abarkan, and M. D. Fontana, "Comparative study of nonlinear optical crystals for electro-optic Q-switching of laser resonators," Opt. Mater., Vol. 26, No. 4, pp. 449–458, Sept. 2004.

[13] B. E. A. Saleh and M. C. Teich, *Fundamentals of Photonics*, 2nd Ed. New York: Wiley, pp. 980–983, 2019.

[14] A. Yariv, *Optical Electronics*. New York: Oxford Univ. Press, pp. 309–343, 1991.

[15] J.F. Nye, *Physical Properties of Crystals: Their Representation by Tensors and Matrices*, Oxford: Clarendon Press, pp. 235–258, 1985.

[16] T.R. Sizer II, I.N. Duling III, C.H. Petras, and S.A. Letzring, "Pockels cell driver," U.S. Patent 4 620 113, Nov. 1986.



Mehdi Keikha received his BSc in Optics and laser engineering from Shahid Bahonar University (SBU) in 2021. He worked as a Master's student at the Femtosecond Lasers Research Laboratory from 2021 to 2024 at Shahid Beheshti University (SBU). His research interests include lasers, amplifiers of pulsed lasers, electronics and nonlinear optics.



Abolfazl Abedi received his MSc in Electrical Engineering in 2016 and his Ph.D. in semiconductor devices in 2020 from Shahid Beheshti University, Tehran, Iran. Since 2024, he has been a faculty member at the Laser and Plasma Research Institute of Shahid Beheshti University, Tehran, Iran. His research interests include optoelectronics, quantum optics, single-photon detectors, and their applications.



Reza Massudi received his BSc from Sharif University of Technology in 1988, his MSc from Isfahan University of Technology in 1992, and his PhD in laser physics from Laval University, Quebec, Canada in 1999. He has been a faculty member of the Laser and Plasma Research Institute, Shahid Beheshti University, Tehran, Iran since 2000. His interests are ultrashort and fiber lasers and their applications, such as biophotonics. He has published different papers in related journals and presented his research works at national and international conferences.

[Downloaded from ijop.ir on 2026-11-23]

THIS PAGE IS INTENTIONALLY LEFT BLANK.

[Downloaded from ijop.ir on 2026-11-23]